CrossMark

Developing constitutive equations of flow stress for hot deformation of AZ31 magnesium alloy under compression, torsion, and tension

Hamed Mirzadeh[1] 🆔

Abstract
A comparative study was carried out on AZ31 (Mg-3Al-1Zn) magnesium alloy to understand the effect of deformation mode on the hot flow stress. Accordingly, the peak flow stress resulted from hot compression, hot tension, and hot torsion tests were correlated to the Zener-Hollomon parameter using the Sellars-McTegart approach. Based on the analysis, by applying the lattice self-diffusion activation energy of magnesium (135 kJ/mol) as the deformation activation energy, the hyperbolic sine exponents were determined to be ∼ 5. Consequently, by consideration of creep exponent of 5, some reliable semi-empirical constitutive equations were proposed for high-temperature deformation of AZ31 alloy and the effect of deformation mode was quantified.

Keywords Hot working · Flow stress · Deformation mode · Thermomechanical processing · Constitutive modeling

Introduction

At elevated temperatures, not only the workability of Mg and its alloys increases as a result of the activation of additional slip systems [1], but also thermomechanical processing can significantly enhance the properties of the casting parts [2]. Therefore, hot deformation processing can be considered as a suitable forming method for magnesium and its alloys. The understanding of the hot deformation behavior of the material under consideration together with the constitutive relations describing material flow (for mathematical simulation) is the prerequisite for industrial applications. As a result, this subject has received a considerable attention [3–8].

The hot deformation studies are usually conducted by simple deformation techniques such as compression, torsion, and tension. Tension often is not able to deliver flow stresses for high strains required in forming processes as a result of instability issues. Compression is also limited to true strains of about 1.5 due to frictional effects [9]. Torsion is capable of simulating multistage hot rolling but results in a radial strain and strain rate gradient, which requires calculation of equivalent surface stress and strain and tangential microstructural examination [9]. It is apparent that the level of achievable strain in these techniques is different. However, what about the flow stress? Researchers around the world use one of these deformation modes to study the constitutive behavior of materials. Therefore, it is interesting to conduct a comparative study on the level of flow stress determined from these techniques. For this purpose, a comparative framework is required to make the comparison reliable.

The commonly used constitutive equation in hot working studies has been proposed by Sellars and McTegart [10] and other researchers [11, 12], which can be expressed as $Z = \dot{\varepsilon}\exp(Q/RT) = A[\sinh(\alpha\sigma)]^{n}$. It can be seen that the Zener-Hollomon parameter (Z) [13, 14] has been related to the flow stress (σ) using the hyperbolic sine function suggested by Garofalo [15]. Based on this equation, hot working has been considered as a thermally activated process and it can be described by strain-rate equations similar to those employed in creep studies.

Conventionally, Q (hot deformation activation energy), A (hyperbolic sine constant), n (hyperbolic sine power), and α (stress multiplier) are considered to be apparent material's parameters by neglecting the underlying mechanisms. Recently, an easy to apply approach in hot deformation studies has been proposed that considers the values of n and Q in the constitutive analysis

✉ Hamed Mirzadeh
hmirzadeh@ut.ac.ir

1 School of Metallurgy and Materials Engineering, College of Engineering, University of Tehran, P.O. Box 11155-4563, Tehran, Iran

based on the creep deformation mechanisms to obtain a more reliable relation [16–20]. This technique has been also extended to make it possible to conduct comparative hot deformation studies and has been successfully applied for hot deformation of Mg alloys to elucidate the effect of alloying elements [21, 22] and deformation mechanisms [23]. Therefore, the same idea might be also applied for the comparison of the different deformation modes.

In the current work, the constitutive behavior of one of the most common Mg alloys (AZ31) with emphasis on the application of creep-based material's parameters will be analyzed to make it possible studying the effect of the deformation mode on the constitutive behavior and hot flow stress based on the obtained values of A and α.

Experimental details

The description of flow stress by the equation $Z = \dot{\varepsilon}\exp(Q/RT) = A[\sinh(\alpha\sigma)]^n$ is incomplete, because no strain for determination of flow stress is specified. Therefore, characteristic stresses that represent the same deformation or softening mechanism for all flow curves, such as steady state, peak, or critical stress for initiation of DRX, should be used in this eq. [5]. In general, the peak stress is the most widely accepted one for finding the hot working constants [16]. Therefore, the peak flow stress (σ_P) data of AZ31 magnesium alloy with nominal composition of Mg – 3 wt% Al – 1 wt% Zn based on hot torsion [24–26], hot compression [27–32], and hot tension [33, 34] tests were taken from the literature with emphasis on the consistency of stress level among different research works that deal with the same deformation technique. The considered flow curves exhibited typical dynamic recrystallization (DRX) behavior [35–38] with a single peak stress followed by a gradual fall toward a steady state stress.

Since the flow data has been taken from the literature and the details of the considered materials and experiments in each research work is different, some other factors such as grain size, texture, and small variations in chemical compositions can affect the level of flow stress. However, the consideration of these parameters is not easy and needs a huge database, which is not the case for the considered material in the current work. Therefore, the following analysis can fairly demonstrate the averaged constitutive behavior of this material for different deformation modes. It should also be noted that the initial grain size is believed to exert little effect on the hot flow stress in hot deformation and in creep when intragranular motion of dislocations is underway but it has a strong influence on the recrystallization process and also on the transition from single peak to cyclic behavior [17, 18, 35, 39, 40].

Results and discussion

Constitutive analyses

As shown in Eq. 1, Z can be related to flow stress in different ways. The power law description of stress is preferred for relatively low stresses. Conversely, the exponential law is suitable for high stresses of power law breakdown regime. However, the hyperbolic sine law can be used for a wide range of temperatures and strain rates [9].

$$Z = \dot{\varepsilon}\exp\left(\frac{Q}{RT}\right) = \begin{cases} A\{\sinh(\alpha\sigma)\}^n \\ A'\sigma^{n'} \\ A''\exp(\beta\sigma) \end{cases} \quad (1)$$

where, A, A', A'', n, n', β and α ($\approx\beta/n'$) are material's constants. The stress multiplier α is an adjustable constant which brings $\alpha\sigma$ into the correct range to make constant temperature curves in $\ln\dot{\varepsilon}$ versus $\ln\{\sinh(\alpha\sigma_P)\}$ plots linear and parallel [9–12, 41]. Taking natural logarithm from both sides of Eq. 1 results in the following expressions:

$$\ln Z = \ln\dot{\varepsilon} + \frac{Q}{R} \times \frac{1}{T} = \begin{cases} \ln A + n\ln\{\sinh(\alpha\sigma)\} \\ \ln A' + n'\ln\sigma \\ \ln A'' + \beta\sigma \end{cases} \quad (2)$$

Based on the Eq. 2, by consideration of peak stresses, the slopes of the plots of $\ln\dot{\varepsilon}$ against $\ln\sigma_P$ and $\ln\dot{\varepsilon}$ against σ_P can be used for obtaining the values of n', β and subsequently $\alpha \approx \beta/n'$. The corresponding plots are shown in Fig. 1, which resulted in the average value of $\alpha \approx 0.01$ MPa^{-1} for all of the considered deformation modes.

According to Eq. 2, the slopes of the plots of $\ln\{\sinh(\alpha\sigma)\}$ against $1/T$ can be used for obtaining the value of Q. The required plots are shown in Fig. 2. The linear regression of the data results in the values of $Q = 135.94$, 138.89, and 139.60 kJ/mol for hot compression, hot torsion, and hot tension data, respectively. These values are close to the value reported for the lattice self-diffusion activation energy of magnesium, which is ~ 135 kJ/mol [17]. Therefore, the value of $Q = 135$ kJ/mol was considered to calculate Z for all of the studied deformation modes. Since the Z parameter expresses the deformation condition (deformation temperature and strain rate), this value is important from the standpoint of comparative analysis.

Based on the hyperbolic sine law shown in Eq. 2, the slope of the plot of $\ln Z$ against $\ln\{\sinh(\alpha\sigma_P)\}$ can be used for obtaining the values of n for the considered deformation modes. The corresponding plots are shown in Fig. 3. This
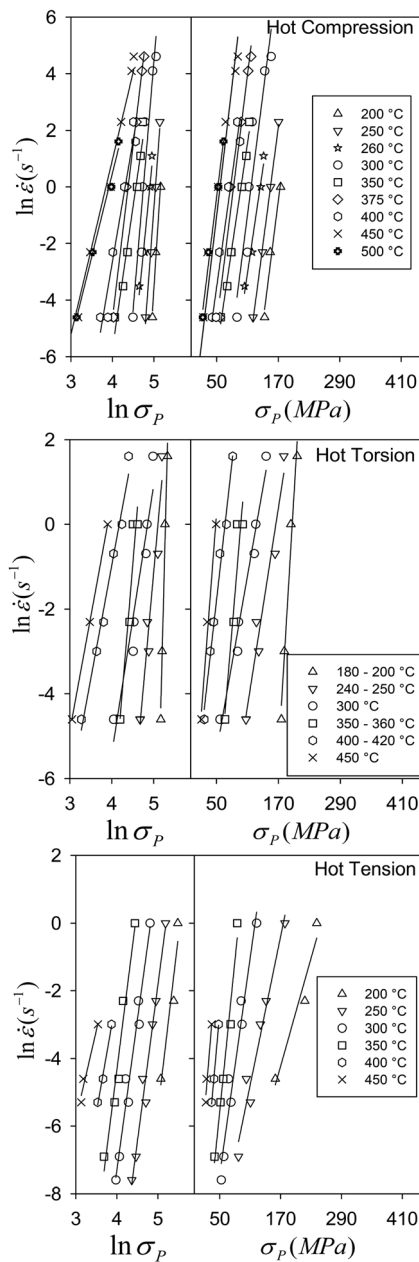
Fig. 1 Plots used to obtain the values of the stress multiplier α

Fig. 2 Plots used to obtain the values of the deformation activation energy Q

of 5 and self diffusion activation energy can be used to describe the appropriate stress [16, 17]. In the current study, the obtained values for n using the self-diffusion activation energy are close to 5, which is consistent with the abovementioned theory. Therefore, the value of n was considered as 5 for all of the studied cases to make the comparison more reliable by using the creep-based material's constants (Q and n).

The effect of the mode of deformation

Figure 4 shows the plots of ln$Z$ against ln{sinh($\alpha\sigma_P$)} by setting $n = 5$. Obviously, the fitted lines are parallel with each other. The linear regression of the data resulted in the values of $A^{0.2} = 170.20$, 177.19, and 143.35 for hot compression, hot torsion, and hot tension data, respectively. As a result, the appropriate constitutive equations to characterize the hot

figure shows that the fitted lines are highly parallel with each other, and hence, have a same slope or equivalently have a same value of n. The linear regression resulted in the values of $n = 5.18$, 5.05, and 5.07 for hot compression, hot torsion, and hot tension data, respectively.

Moreover, as it is evident from Eq. 2, the intercepts of the fitted lines represent the values of ln$A$. Subsequently, the linear regression of the data resulted in the values of $A^{0.2} =$ 140.134, 163.367, and 138.656 for hot compression, hot torsion, and hot tension, respectively. It has been shown that when the deformation is controlled by the glide and climb of dislocations (climb-controlled creep), a constant exponent (n)
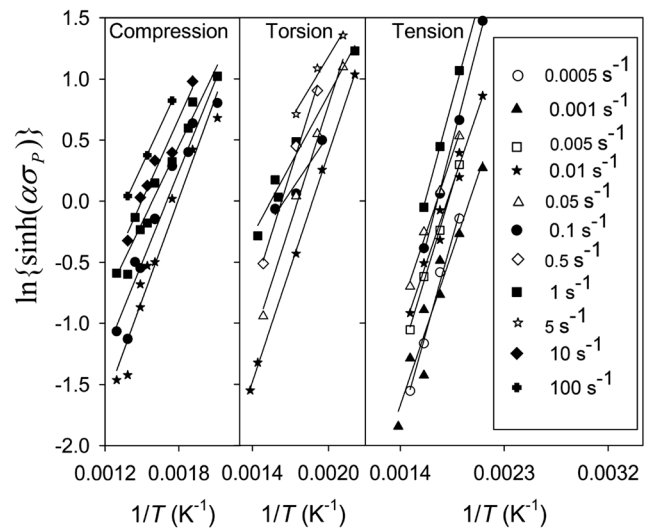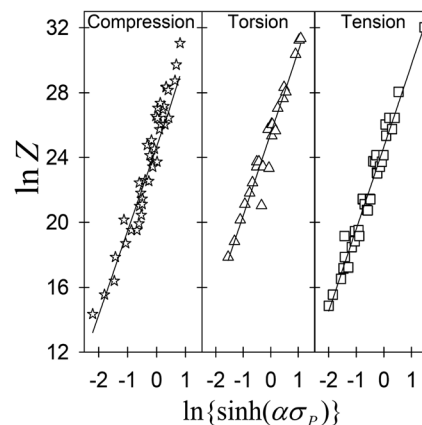

Fig. 3 The analyses based on the hyperbolic sine law using $Q = 135$ kJ/mol and by consideration of apparent values of n for each deformation mode
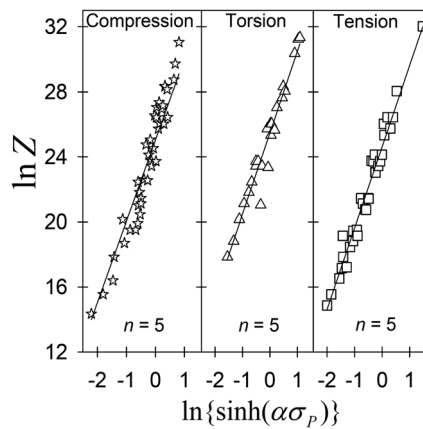
Fig. 4 The analyses based on the hyperbolic sine law using $Q = 135$ kJ/mol and by setting $n = 5$ for each deformation mode

Fig. 5 Power law constitutive analysis

deformation behavior of AZ31 alloy can be expressed as follows:

$$Z = \dot{\varepsilon}\exp\left(\frac{135000}{RT}\right)$$
$$= \begin{cases} 170.20^5\left\{\sinh(0.01\sigma_p)\right\}^5 \Leftrightarrow Compression \\ 177.19^5\left\{\sinh(0.01\sigma_p)\right\}^5 \Leftrightarrow Torsion \\ 143.35^5\left\{\sinh(0.01\sigma_p)\right\}^5 \Leftrightarrow Tension \end{cases} \quad (3)$$

Since the values of $n = 5$, $Q = 135$ kJ/mol, and $\alpha = 0.01$ MPa^{-1} were used in the hyperbolic sine equation for all of the investigated cases, the differences in constitutive behaviors can be deduced solely from the values of A. Based on Eq. 1, it is clear that a higher A gives a lower flow stress: $\sigma = \{\sinh^{-1}(Z/A)^{1/n}\}/\alpha$. Therefore, the hot tension test has resulted in a somewhat higher peak flow stress levels in this case. However, the level of flow stresses form the compression and torsion tests are close to each other, which is an interesting finding because these two techniques are the most widely used ones in hot deformation studies.

It should be noted that while the consideration of the apparent values of n, Q, and α (which somehow deviate from the considered values) may result in a better fit to experimental data, but the possibility of elucidating the effect of the mode of deformation on the hot working behavior will be lost. Therefore, the used approach in the present work can be considered as a versatile tool in comparative hot working studies.

The power law constitutive analyses

Based on the power law description of flow stress as shown by Eq. 2, the slope and the intercept of the plot of $\ln Z$ against $\ln\sigma_P$ can be used for obtaining the values of n' and A', respectively. The corresponding plots for flow stress data, that have not exhibited the power law breakdown, are shown in Fig. 5, which shows that the fitted lines are highly parallel with each
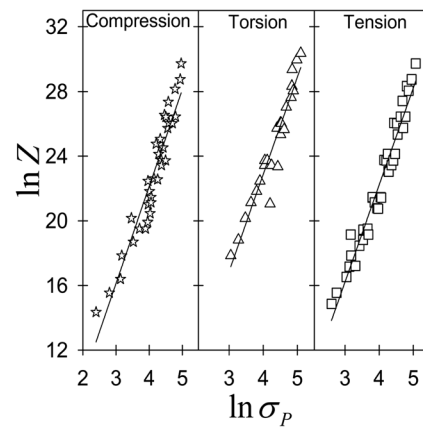
other and hence have a same slope ($n' \approx 6$). Therefore, the power law description for the hot deformation of AZ31 alloy can be summarized as follows:

$$Z = \dot{\varepsilon}\exp\left(\frac{135000}{RT}\right) = \begin{cases} 0.154\sigma_P^6 \Leftrightarrow Compression \\ 0.327\sigma_P^6 \Leftrightarrow Torsion \\ 0.166\sigma_P^6 \Leftrightarrow Tension \end{cases} \quad (4)$$

Or equivalently

$$\sigma_P = \begin{cases} 1.365Z^{0.166} \Leftrightarrow Compression \\ 1.205Z^{0.166} \Leftrightarrow Torsion \\ 1.349Z^{0.166} \Leftrightarrow Tension \end{cases} \quad (5)$$

Based on the power law equations shown by Eq. 5, the hot compression and hot tension tests have resulted in the highest stress levels, while based on the hyperbolic sine law (Eq. 3), only the hot tension test was found to yield the highest flow stress. This can be ascribed to the fact that for the analyses based on the power law some of the flow stress data corresponding to the power law breakdown regime have been neglected. Anyway, Eq. 5 clearly shows that the level of the peak flow stresses resulted from the three deformation modes are not significantly different.

Conclusively, by developing these reliable constitutive equations for high-temperature deformation of AZ31 alloy, the effect of deformation mode can be quantified. This approach can be also applied to different materials and other deformation modes.

Summary

In summary, it was revealed that the exponent of $n = 5$ and the self-diffusion activation energy of magnesium (135 kJ/mol) as the hot deformation activation energy (Q) can be used in the

hyperbolic sine equation of $Z = \dot{\varepsilon}\exp(Q/RT) = A\{\sinh(\alpha\sigma_P)\}^n$ to describe the peak stress of AZ31 magnesium alloy deformed under hot compression, hot torsion, and hot tension tests. This simple approach reduces the number of constants that depend on the deformation mode. As a result, the used method in the present work can be considered as a versatile tool in hot working studies for comparative purposes and for elucidating the effect of the deformation mode.

Compliance with ethical standards

Conflict of interest The author declares that he has no conflict of interest.

Publisher's Note Springer Nature remains neutral with regard to jurisdictional claims in published maps and institutional affiliations.

References

1. Barnett MR (2001) Influence of deformation conditions and texture on the high temperature flow stress of magnesium AZ31. J Light Met 1(3):167–177
2. Pourbahari B, Mirzadeh H, Emamy M (2017) Toward unraveling the effects of intermetallic compounds on the microstructure and mechanical properties of mg–Gd–Al–Zn magnesium alloys in the as-cast, homogenized, and extruded conditions. Mater Sci Eng A 680:39–46
3. Liang R, Khan AS (1999) A critical review of experimental results and constitutive models for BCC and FCC metals over a wide range of strain rates and temperatures. Int J Plast 15(9):963–980
4. Lin YC, Chen XM (2011) A critical review of experimental results and constitutive descriptions for metals and alloys in hot working. Mater Des 32(4):1733–1759
5. Anand L (1985) Constitutive equations for hot-working of metals. Int J Plast 1(3):213–231
6. Mirzadeh H (2015) A simplified approach for developing constitutive equations for modeling and prediction of hot deformation flow stress. Metall Mater Trans A 46(9):4027–4037
7. Lin J, Liu Y (2003) A set of unified constitutive equations for modelling microstructure evolution in hot deformation. J Mater Process Technol 143-144:281–285
8. Nedoushan RJ, Farzin M, Banabic D (2014) Simulation of hot forming processes: using cost effective micro-structural constitutive models. Int J Mech Sci 85:196–204
9. McQueen HJ, Ryan ND (2002) Constitutive analysis in hot working. Mater Sci Eng A 322(1-2):43–63
10. Sellars CM, McTegart WJ (1966) On the mechanism of hot deformation. Acta Metall 14(9):1136–1138
11. McQueen HJ, Wong WA, Jonas JJ (1967) Deformation of aluminium at high temperatures and strain rates. Can J Phys 45(2):1225–1234
12. Uvira JL, Jonas JJ (1968) Hot compression of Armco iron and silicon steel. Trans Metall Soc AIME 242:1619–1626
13. Zener C, Hollomon JH (1944) Effect of strain rate upon plastic flow of steel. J Appl Phys 15(1):22–32
14. Dieter GE (1988) Mechanical metallurgy, 3rd edn. McGraw-Hill, New York
15. Garofalo F (1963) An empirical relation defining the stress dependence of minimum creep rate in metals. Trans Metall Soc AIME 227:351–356
16. Mirzadeh H, Cabrera JM, Najafizadeh A (2011) Constitutive relationships for hot deformation of austenite. Acta Mater 59(16):6441–6448
17. Langdon TG (2005) An analysis of flow mechanisms in high temperature creep and Superplasticity. Mater Trans 46(9):1951–1956
18. Mukherjee AK (2002) An examination of the constitutive equation for elevated temperature plasticity. Mater Sci Eng A 322(1-2):1–22
19. Cabrera JM, Al Omar A, Prado JM, Jonas JJ (1997) Modeling the flow behavior of a medium carbon microalloyed steel under hot working conditions. Metall Mater Trans A 28(11):2233–2244
20. Galiyev A, Sitdikov O, Kaibyshev R (2003) Deformation behavior and controlling mechanisms for plastic flow of magnesium and magnesium alloy. Mater Trans 44(4):426–435
21. Mirzadeh H (2014) Constitutive analysis of mg–Al–Zn magnesium alloys during hot deformation. Mech Mater 77:80–85
22. Mirzadeh H (2015) Constitutive behaviors of magnesium and mg–Zn–Zr alloy during hot deformation. Mater Chem Phys 152:123–126
23. Mirzadeh H, Roostaei M, Parsa MH, Mahmudi R (2015) Rate controlling mechanisms during hot deformation of mg–3Gd–1Zn magnesium alloy: dislocation glide and climb, dynamic recrystallization, and mechanical twinning. Mater Des 68:228–231
24. Beer AG, Barnett MR (2006) Influence of initial microstructure on the hot working flow stress of mg–3Al–1Zn. Mater Sci Eng A 423(1-2):292–299
25. Myshlyaev MM, McQueen HJ, Mwembela A, Konopleva E (2002) Twinning, dynamic recovery and recrystallization in hot worked mg–Al–Zn alloy. Mater Sci Eng A 337(1-2):121–133
26. Spigarelli S, El Mehtedi M (2010) Creep as an extension of hot working: a unified approach to high temperature deformation of AZ31 alloy. Mater Sci Eng A 527(21-22):5708–5714
27. Gall S, Huppmann M, Mayer HM, Muller S, Reimers W (2013) Hot working behavior of AZ31 and ME21 magnesium alloys. J Mater Sci 48(1):473–480
28. Kawalla R, Stolnikov A (2004) Deformation behaviour and microstructure development of magnesium AZ31 alloy during hot and semi-hot deformation. Adv Eng Mater 6(7):525–529
29. Luan J, Sun C, Li X, Zhang Q (2014) Constitutive model for AZ31 magnesium alloy based on isothermal compression test. Mater Sci Technol 30(2):211–219
30. Poletti C, Dieringa H, Warchomicka F (2009) Local deformation and processing maps of as-cast AZ31 alloy. Mater Sci Eng A 516(1-2):138–147
31. Sanjari M, Farzadfar SA, Jung IH, Essadiqi E, Yue S (2012) Influence of strain rate on hot deformation behaviour and texture evolution of AZ31B. Mater Sci Technol 28(4):437–447
32. Zhong T, Rao KP, Prasad YVRK, Gupta M (2013) Processing maps, microstructure evolution and deformation mechanisms of extruded AZ31-DMD during hot uniaxial compression. Mater Sci Eng A 559:773–781
33. Deng J, Lin YC, Li S, Chen J, Ding Y (2013) Hot tensile deformation and fracture behaviors of AZ31 magnesium alloy. Mater Des 49:209–219
34. Liu Z, Xing S, Bao P, Li N, Yao S, Zhang M (2010) Characteristics of hot tensile deformation and microstructure evolution of twin-roll cast AZ31B magnesium alloys. Trans Nonferrous Metals Soc China 20(5):776–782
35. Sakai T, Jonas JJ (1984) Dynamic recrystallization: mechanical and microstructural considerations. Acta Metall 32(2):189–209
36. Saadatkia S, Mirzadeh H, Cabrera JM (2015) Hot deformation behavior, dynamic recrystallization, and physically-based constitutive modeling of plain carbon steels. Mater Sci Eng A 636:196–202
37. Mirzadeh H, Najafizadeh A (2010) Prediction of the critical conditions for initiation of dynamic recrystallization. Mater Des 31(3):1174–1179

38. Roostaei M, Parsa MH, Mahmudi R, Mirzadeh H (2015) Hot compression behavior of GZ31 magnesium alloy. J Alloys Compd 631: 1–6

39. Humphreys FJ, Hatherly M, *Recrystallization and* Related annealing phenomena, 2nd ed., Elsevier, Oxford, UK, 2004

40. Mirzadeh H (2015) Constitutive description of 7075 aluminum alloy during hot deformation by apparent and physically-based approaches. J Mater Eng Perform 24(3):1095–1099

41. Phaniraj C, Samantaray D, Mandal S, Bhaduri AK (2011) A new relationship between the stress multipliers of Garofalo equation for constitutive analysis of hot deformation in modified 9Cr–1Mo (P91) steel. Mater Sci Eng A 528(18):6066–6071